Journal of the Korean Physical Society, Vol. 64, No. 4, February 2014, pp. 547∼553

Effect of Van der Waals Interaction on the Structural and Cohesive Properties of Black Phosphorus

Hanchul Kim*
Department of Physics, Sookmyung Women's University, Seoul 140-742, Korea

(Received 14 January 2014)

We investigated the structural and the binding properties of black phosphorus (black-P) by employing density functional theory (DFT) calculations in combination with various implementations of the van der Waals (vdW) interaction. Both the binding energy curve of the two isolated puckered layers and the equation of states of the bulk black-P suggest that the conventional generalized gradient approximation (GGA) functional is incapable of describing the interlayer vdW interaction. From the comparison of the seven different vdW implementations, the appropriate vdW schemes in describing layer-structured black-P are found to be either the Grimme's dispersion correction (DFT-D2) or the optB86b vdW denisty-functional approach.

PACS numbers: 61.50.Lt, 61.66.Bi, 64.30.+t, 71.15.Nc
Keywords: Density functional theory, Van der Waals interaction, Black phosphorus, Layered structure
DOI: 10.3938/jkps.64.547

I. INTRODUCTION

Black phosphorus (black-P) has many benefits as an anode material for lithium ion batteries because of its atomic and electronic properties. A composite of black-P and carbon has been demonstrated to result in an enhanced electrochemical discharge/charge efficiency with a good cyclability [1]. Due to the layered structure, black-P can guarantee large specific capacity for lithium ion batteries. In addition, the semiconducting nature of black-P with a small band gap (0.19 eV) will allow many potential applications in electronics technology [2].

In nature, phosphorus is found in three allotropic forms with different dimensionalities, reminiscent of carbon allotropes such as the zero-dimensional (0D) fullerene, the one-dimensional (1D) carbon nanotube, and the two-dimensional (2D) graphene. The three phosphorus allotropes are classified by their characteristic colors. White phosphorus (white-P) is a reactive molecular crystal whose building unit is the 0D P_4 molecule. White-P is further classified into three structural modifications (α-, β-, and γ-P_4) due to different arrangements of P_4 molecules [3–5]. Red phosphorus (red-P) is made up of 1D polymeric chains. Finally, the most stable allotrope, black-P, is characterized by a staggered stacking of puckered layers (PLs) [6]. Judging from the structural building units, the van der Waals (vdW) interaction seems to play an important role in the structural and the thermodynamic properties of P allotropes.

Density functional theory (DFT) [7, 8] calculations have been successfully applied in describing the covalent and the ionic bonds in various molecules and crystals and has become the preferred tool in condensed matter physics. However, it has experienced problems in predicting the structural and the thermodynamic properties of weakly-bound molecular aggregates because the DFT is not capable of describing the long-range dynamical correlation between induced dipoles. Many efforts have been made to remedy this shortcoming. One class of approaches is to devise non-local density functionals describing the vdW interaction and is called the vdW density-functional (vdW-DF) scheme [9–15]. Klimĕs *et al.* showed that the accuracy of the original vdW-DF could be improved by using alternative generalized-gradient-approximation (GGA) exchange components and proposed three variations of vdW-DF, optPBE, optB88, and optB86b [16, 17]. The other class is the semi-empirical approach to describe the vdW interaction by adding a pairwise interatomic dispersion correction (C_6R^{-6}) [18–22]. Within this class, depending on the way in which the C_6 coefficients are determined, the approaches can be further divided into the parametrized dispersion corrections, where the most widely used is the so-called DFT-D method by Grimme *et al.* [18–21], and the parameter-free methods represented by a recent work done by Tkatchenko and Scheffler (TS) [22].

The vdW forces are very weak compared to chemical interactions, but they play a crucial role in weakly-bound systems such as noble-gas elements and non-polar molecules [23], π-electron systems like carbon allotropes

*E-mail: hanchul@sookmyung.ac.kr

Table 1. Binding properties of the two PLs from LDA, PBE, and different DFT+vdW calculations: equilibrium distance d_0 ($\AA$) and binding energy ε_b (eV/P_4).

	LDA		PBE							
	w/o vdW	D2	w/o vdW	D2	TS	DF	DF2	optPBE	optB88	optB86b
d_0	2.93	2.89	3.42	3.09	3.32	3.53	3.51	3.30	3.19	3.09
ε_b	0.17	0.34	0.03	0.17	0.19	0.15	0.17	0.20	0.22	0.24

(C_{60}, carbon nanotubes, graphite, *etc.*), and organic molecules in biological systems [11,12]. As a few examples, the interaction of the in-plane benzene molecules [24], the interactions between benzene and naphthalene molecules on graphite [25], and the interlayer binding in graphite [26] were studied to verify that the vdW interaction was crucial in stabilizing such materials. Very recently, the vdW-DF method was applied to bulk crystals, for which the vdW forces had previously been thought not to be that important [17].

To our knowledge, there has not been a comprehensive investigation of the role of the vdW interaction in P allotropes except for our recent study on the intermolecular interaction between P_4 molecules [27]. We found that the GGA predicted too weak an intermolecular binding whereas the local density approximation (LDA) results in too strong an intermolecular binding. Only with the use of the dispersion correction (DFT-D2, a modified version of DFT-D) in combination with the GGA, was a reasonable binding property obtained. As for black-P, early theoretical studies were focussed either on the electronic structure [28, 29] or on the structural phase transitions [30]. In a few recent studies, the researchers tried to consider the effect of the vdW interaction [31–33]. Du *et al.* [31] claimed that the Perdew-Wang GGA functional (PW91) [34] described the vdW interaction between two PLs with the interlayer distance of 5.1 Å and the binding energy of 0.06 eV/P_4, which is an incorrect proposition because the interlayer vdW distance in black-P is about 3.1 Å [35, 36]. Prytz and Flage-Larsen [32] examined the Heyd-Scuseria-Ernzerhof (HSE03) [37] and Perdew-Burke-Ernzerhof (PBE0) [38] hybrid functionals, and found that neither hybrid functionals could properly describe the vdW interaction in black-P. The HSE03 predicted an interlayer vdW distance (3.48 Å) shorter than the GGA value (3.52 Å), which is much larger than the experimental value (3.1 Å), and the PBE0 failed to relax the structure. Very recently, Appalakondaiah and coworkers [33] investigated the effect of the vdW interaction on the structural and the elastic properties of black-P. Among the studied semi-empirical vdW corrections, the DFT-D2 scheme [19] was found to yield structural parameters which are in closest agreement with experimental data.

In this work, we investigated the effect of the vdW interaction on the structural and the thermodynamical properties of black-P. First, we calculated the binding energy curve of the two PLs by employing various implementations of the vdW interaction. Then, we calculated the equation of states of black-P, where one can obtain the fundamental structural, elastic, and cohesive properties. Based on those calculated results, we were able to address the efficacy of different vdW implementations in describing the inter-PL interaction of black-P.

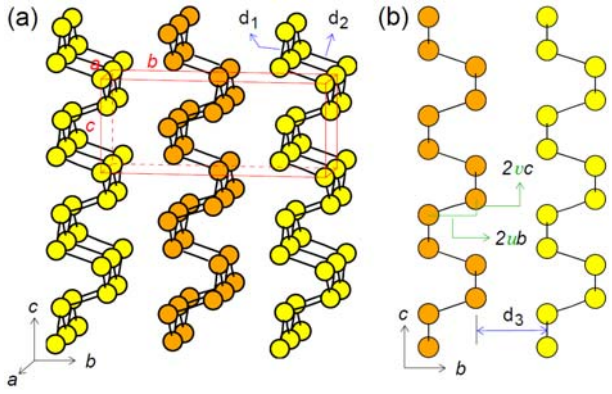

Fig. 1. (color online) (a) Structure of black-P showing the three lattice constants, a, b, and c, and the orthorhombic cell. d_1 and d_2 are the in-plane and the out-of-plane bonds, respectively. (b) Side view of black-P where the interlayer vdW distance d_3 and the internal coordinates u and v are defined. The alternating staggered PLs are represented by using different colors for distinction.

II. COMPUTATIONAL METHODS

We used the Vienna *Ab initio* Simulation Package (VASP) [39–42] to perform the DFT calculations with the vdW interaction, as well as the conventional DFT calculations. We employed two semi-empirical dispersion corrections, DFT-D2 [19] and TS [22], the original vdW-DF scheme of Dion *et al.* [10] and its modified version (vdW-DF2) [15], and three variations of vdW-DF (optPBE, optB88, and optB86b) [16, 17]. The phosphorus atoms were represented by using the projector-augmented-wave potential [43, 44]. The exchange-correlation was described within the Ceperley-Alder scheme [45] for the LDA and within the Perdew-Burke-Ernzerhof (PBE) scheme [46] for the GGA. An orthorhombic cell, which is shown in Fig. 1(a) as a red rectangular parallelepiped and is twice as large as the primitive unit cell, was used for the calculations of bulk

black-P. To investigate the binding properties of the two PLs, we used a 1 × 2 × 1 supercell that was doubled in the normal direction [b in Fig. 1(a)] to the PLs. A kinetic energy cutoff of 400 eV was used for the expansion of the wave functions. The momentum-space integrations were approximated using a k-point mesh equivalent to the 12 × 4 × 8 Monkhorst-Pack grid [47] of orthorhombic black-P. These parameters guarantee an energy accuracy of 1 meV/atom.

III. RESULTS AND DISCUSSIONS

Black-P has an orthorhombic symmetry with eight P atoms in the orthorhombic unit cell making a layered structure, as shown in Fig. 1, similarly to that of graphite when it comes to the interlayer interaction. Differently from carbon, because P has five valence electrons, each P atom prefers to have three bonds that do not lie on a single plane. As a consequence, the atomic layers in black-P are puckered. Each PL can be viewed as a bilayer of two parallel atomic planes. On each plane, P atoms constitute a zigzag chain running along the a axis. Within a PL, P atoms form covalent bonds with three nearest neighbors (two on the same plane and one on a neighboring plane); the in-plane bond length (d_1) is around 2.22 Å, and the out-of-plane bond length (d_2) is around 2.28 Å. The distance between two adjacent PLs is known to be about 3.07 Å, which is significantly longer than the length of the P-P covalent bond [36]. The atoms in the orthorhombic cell are located at the following points:

$$\pm\,(0, ub, vc)\,, \qquad \pm\left(\frac{a}{2}, ub, (\frac{1}{2}-v)c\right),$$
$$\pm\left(0, (\tfrac{1}{2}+u)b, (\tfrac{1}{2}-v)c\right), \quad \pm\left(\frac{a}{2}, (\frac{1}{2}+u)b, vc\right).$$

We note that the orthorhombic cell depicted in Fig. 1(a) is not the primitive unit cell, but is twice as large as the primitive unit cell. The lattice vectors for the primitive cell can be written as

$$\mathbf{a_1} = \frac{1}{2}(\mathbf{a}-\mathbf{b}),\ \ \mathbf{a_2} = \tfrac{1}{2}(\mathbf{a}+\mathbf{b}),\ \ \mathbf{a_3} = \mathbf{c},$$

and the coordinates of the four atoms in the primitive cell are

$$\pm(-u\mathbf{a_1} + u\mathbf{a_2} + v\mathbf{a_3}),$$
$$\pm\left((\tfrac{1}{2}-u)\mathbf{a_1} + (\tfrac{1}{2}+u)\mathbf{a_2} + (\tfrac{1}{2}-v)\mathbf{a_3}\right).$$

First, we investigated the binding of two staggered PLs. We placed two PLs in an orthorhombic cell that was twice longer along the b axis than the orthorhombic cell of black-P [Fig. 1(a)] and performed the total energy calculations by varying the distance d between the two PLs as shown in Fig. 2(c). The binding energy curves obtained from conventional LDA and PBE calculations and from seven different DFT+vdW calculations are plotted in Fig. 2. The characteristic parameters of the binding energy curve, the equilibrium distance (d_0) and the binding energy (ε_0) defined in Fig. 2(b), are listed in Table 1.

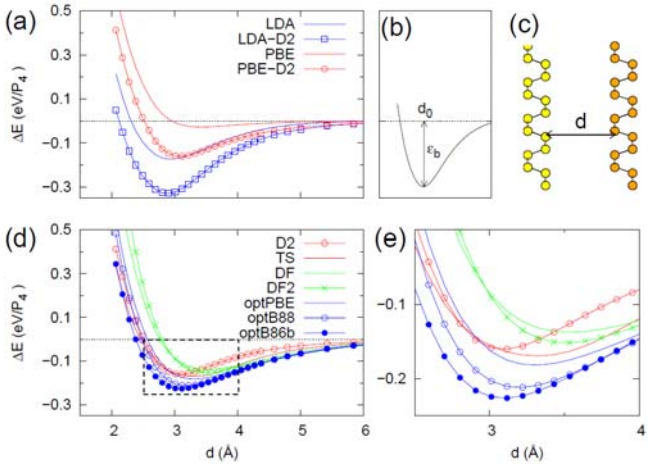

Fig. 2. (color online) Binding energy curves of two PLs. (a) Cases of LDA, LDA-D2, PBE, and PBE-D2, (b) model binding energy curve showing the equilibrium distance d_0 and the binding energy ε_0, (c) schematic diagram of two PLs indicating the interlayer distance d, (d) the binding energy curves from seven vdW-corrected calculations, and (e) magnified binding energy curves near equilibrium corresponding to the dashed area in (d).

Figure 2(a) compares the LDA, LDA-D2, PBE, and PBE-D2 binding energy curves to show the characteristic differences. Evidently, the PBE predicts a very weak binding between the PLs with a shallow well of 0.03 eV/P_4 and an equilibrium distance of 3.42 Å. In contrast, the LDA predicts a stronger binding with ε_0 = 0.17 ev/P_4 and a shorter equilibrium distance of d_0 = 2.93 Å. With the added contribution of the dispersion correction, the binding energy is increased, and the equilibrium distance is shortened for both the LDA and the PBE. The effect of the dispersion correction is more prominent in the case of the PBE, and the equilibrium distance (3.09 Å) is almost the same as the interlayer vdW gap (3.07 Å) in black-P. On the other hand, the binding energy of the LDA-D2, 0.34 eV/P_4, suggests too strong a binding. These observations are similar to the trends found in the interaction between P_4 molecules [27].

The results from different PBE+vdW calculations are compared in Figs. 2(d) and 2(e). The original vdW-DF and its modification (vdW-DF2) were found to result in a larger equilibrium separation ($d_0 \geq$ 3.50 Å) between the PLs, which is even larger than the PBE value of 3.42 Å. This is in agreement with the results for crystalline solids in which the original vdW-DF tends to overestimate the lattice constants [17]. As for the semi-empirical dispersion corrections, the TS scheme reveals a slightly deeper and longer binding tendency than the PBE-D2 method. This is in contrast with a previous

Table 2. Equilibrium structural parameters of black phosphorus obtained from the equation of states in Fig. 3. Shown are the equilibrium volume of the primitive cell (V_{pc}) and its relative error with respect to the experimental volume [36], the bulk modulus (B_0) and its pressure derivative (B'), and the cohesive energies of black phosphorus (E_c) and P_4 molecule ($E_c^{P_4}$).

		V_{pc} ($\AA^3$)	$\Delta V_{pc}/V_{pc}^{exp}$ (%)	B_0 (GPa)	B'	Cohesive energy (eV/P_4)	
						E_c	$E_c^{P_4}$
Exp.	Ref. 36	75.972	–	32.5	6.11	–	–
	Ref. 48	–	–	36.0	4.50	–	–
LDA	Ref. 30	77.726	2.4	32.6	5.55	–	–
	w/o vdW	69.641	−8.2	27.8	6.97	18.072	16.346
	D2	68.160	−10.2	35.5	3.83	18.944	16.348
PBE	w/o vdW	85.421	12.6	7.2	15.06	13.949	13.448
	D2	76.995	1.5	27.5	7.56	14.744	13.451
	TS	79.709	5.0	16.6	1.80	14.640	13.449
	DF	89.779	18.3	14.9	8.12	13.483	12.549
	DF2	90.868	19.7	19.5	8.04	13.108	12.142
	optPBE	82.973	9.3	20.2	6.22	14.705	13.372
	optB88	79.987	5.4	24.3	6.56	15.119	13.577
	optB86b	76.133	0.3	25.5	7.25	15.634	14.005

publication where the binding properties of two in-plane benzene molecules were calculated to be almost identical for both the PBE-D2 and the TS schemes [24]. This may indicate that the agreement between PBE-D2 and TS for benzene molecules is a special observation, but not a general tendency.

Among the three variations to the original vdW-DF, the binding strength is increased in the order of optPBE, optB88, and optB86b, as seen in the increasing binding energy (from 0.20 to 0.24 eV/P_4) and the decreasing equilibrium distance (from 3.30 to 3.09 Å). Interestingly, the optPBE results are similar to the semi-empirical TS case. The optB86b equilibrium distance is identical to that of PBE-D2 with a slightly enhanced binding energy by 0.07 eV/P_4. Considering that the experimental interlayer vdW gap of black-P is 3.07 Å, both the semi-empirical PBE-D2 and the vdw-DF optB86b methods seem to be more efficient than the other vdW implementations in describing the vdW interaction of phosphorus PLs.

In order to investigate the structural and the cohesive properties of black-P and the effect of vdW interaction, we performed total energy calculations by varying the cell volume. The resulting volume *vs.* cohesive energy curve is the so-called equation of states, from which we can obtain the basic structural parameters, for instance, theoretical equilibrium lattice constants, the bulk modulus, the pressure derivative of the bulk modulus, and the equilibrium cohesive energy. The calculations were done in two different way: one is a constrained calculation (□ in Fig. 3) where the shape of the orthorhombic cell is unchanged (*i.e.*, only isotropic contractions or expansions are allowed), and the other is the variable-cell-shape calculations (• in Fig. 3) allowing a full relaxation of the stress. At first thought, these calculations seem to result in the same equation of states. However, in reality, they are not the same, especially for highly-anisotropic materials like layered black-P. These two sets of calculations for the LDA, LDA-D2, PBE, and the PBE-D2 are plotted in Figs. 3(a)-3(b).

The prominent feature shared by both LDA and PBE calculations and by their dispersion-corrected calculations is that the constrained equation of states has a larger curvature than the unconstrained equation of states. In other words, the unconstrained calculation predicts an elastically softer structure. This evidences that anisotropic black-P prefers a change in the cell shape away from the equilibrium volume. Comparing the LDA and the LDA-D2 equations of states, the equilibrium volume of the LDA-D2 is smaller than that of the LDA (which is already smaller than the experimental cell volume due to the typical over-binding nature of the LDA). This is due to the additional contribution of the dispersion forces to the interatomic attraction. As for the PBE and the PBE-D2, because the PBE is nearly incapable of giving a proper vdW description, as seen in Fig. 2(a), the equation of states curve becomes almost flat for large cell volumes. This suggests that one has to include the vdW correction when using the PBE exchange-correlation functional.

Because we have established the over-binding tendency of the LDA, the importance of the cell-shape relaxation, and the necessity of the vdW correction for the PBE, we will focus on the efficacy of the various vdW implementations, in combination with the PBE functional, by examining the variable-cell-shape calculations. The resulting equations of states are plotted in Fig. 3(c). One thing to note is that the original vdW-DF and vdW-DF2 predict too large an equilibrium primitive cell volume, ∼90 $\AA^3$, which is about 20% larger than the experimental value

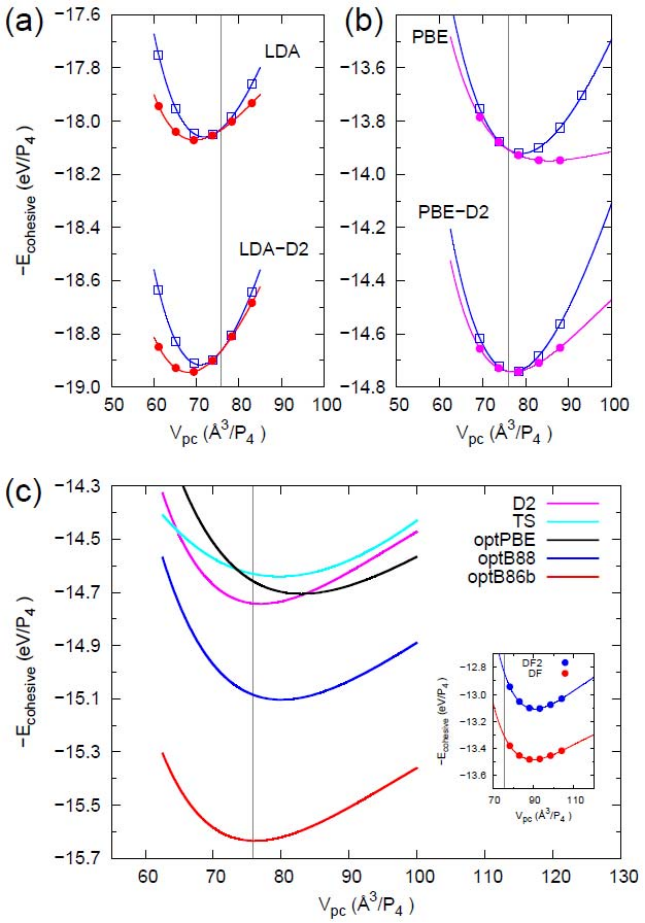

Fig. 3. (color online) Equations of states of black-P from different vdW implementations: (a) LDA and LDA-D2, (b) PBE and PBE-D2, and (c) PBE-D2, TS, optPBE, optB86b, and optB88. The inset in (c) shows the results for vdW-DF and vdW-DF2. Open squares (□) in (a) and (b) are the results from constrained calculations whereas the solid circles (•) are the results from the variable-cell-shape calculations (see text). The vertical lines indicate the experimental primitive cell volume.

in Ref. 36. This is expected because the interlayer interaction in Fig. 2(e), as well as the results in Ref. 17, have already shown the under-binding nature of the original vdW density functionals.

Among the five equations of states in Fig. 3(c), the PBE-D2 and the optB86b reproduce the experimental primitive cell volume better than the other vdW corrections. As shown in Table 2, the relative errors in the cell volume are about 1.5% and 0.3% for the PBE-D2 and the optB86b, respectively. The TS scheme yields about 5% larger cell volume, following the same tendency as we saw in the interlayer interaction [Fig. 2(e) and Table 1]. The results from the variations of vdW-DF are again in accord with the trend observed in the interlayer interaction: the optB86b showing the most binding nature, followed by the optB88 and then by the optPBE with about a 9.3% error.

Regarding the bulk modulus in Table 1, all PBE-based values are smaller than the experimental value. Neglecting the results of the vdW-DF and the vdW-DF2, the most-deviating value occurs for the TS scheme. This implies that the TS vdW correction predicts a black-P that is too soft. Interestingly, the vdW implementation with a larger primitive cell volume tends to yield a smaller bulk modulus, because a larger volume corresponds to a structure with more room for atomic movement and a larger-volume structure is more easily compressible. The cohesive energies of black-P and of the P_4 molecule follow the same tendency as the cell volume does. That is, a smaller cell volume corresponds to a larger cohesive energy and a larger cell volume to a smaller cohesive energy.

Detailed structural parameters obtained from the equations of states are listed in Table 3. We would like to focus on the structural parameters for the PBE-D2 and the optB86b, which yield the cell volumes that best agree with the experimental values. The experimental lattice constants [36] are well reproduced by using both the PBE-D2 and the optB86b, with the largest error being $\sim 1\%$ for c. The absolute errors in the internal coordinates (u and v) are calculated to be smaller than $\sim 3\%$. As for the in-plane (d_1) and the out-of-plane (d_2) bond lengths and the vdW gap (d_3), both d_1 and d_2 show errors less than 1%, and d_3 shows an error less than 3%. It is worth while to note that the out-of-plane bond length (d_2) is slightly contracted whereas the interlayer vdW gap is increased compared with the corresponding experimental values. For other PBE-based vdW implementations, the interlayer vdW gap is much more overestimated, showing a relative error $\geq 10\%$. The successful prediction of the structural and the cohesive properties with both the PBE-D2 and the optB86b for black-P is reminiscent of the description of the PBE-D2 being more reliable than that of the LDA for white-P (β-P_4) [27].

IV. SUMMARY AND CONCLUSION

We have performed DFT calculations on black-P with PLs by employing both the semi-empirical dispersion corrections (DFT-D2 and TS) and the vdW density-functional methods (original vdw-DF, vdw-DF2, and three further variations such as optPBE, optB88, and optB86b) to investigate the effect of the vdW interaction on the structural and the cohesive properties. The binding energy curve of two isolated PLs shows that the PBE marginally develops a very shallow and distant potential well. Among different vdW schemes, both the PBE-D2 and the optB86b are found to be better in fixing the shortcomings of the conventional PBE functional. Similarly, the equations of states for bulk black-P suggest that the PBE-D2 and the optB86b are best for reproducing the experimental structural parameters. Our results confirm that the PBE with a proper dispersion

Table 3. Equilibrium structural parameters of black phosphorus. Lattice constants (a, b, c), internal degrees of freedom (u, v), and bond lengths defined in Fig. 1 are compared with the previous experimental and theoretical values.

		Lattice constants (Å)			Internal coordinates		Bond length (Å)		
		a	b	c	u	v	d_1	d_2	d_3
Exp.	Ref. 35	3.314	10.478	4.376	0.1017	0.0806	2.224	2.244	3.108
	Ref. 36	3.313	10.473	4.374	0.1034	0.0806	2.223	2.278	3.071
	Ref. 49	3.320	10.368	4.315	0.1044	0.0821	2.204	2.278	3.019
Previous calc.	LDA [30]	3.339	10.610	4.388	0.1020	0.0840	2.216	2.287	3.141
	PW91 [31]	3.348	10.587	4.422	0.1011	0.0821	2.238	2.261	3.153
	LDA [32]	3.310	10.551	4.131	0.1064	0.0710	2.220	2.245	2.905
	PBE [32]	3.307	11.269	4.555	0.0990	0.0866	2.225	2.261	3.516
	HSE03 [32]	3.284	11.135	4.527	0.0937	0.0879	2.202	2.234	3.481
LDA	w/o vdW	3.305	10.192	4.135	0.1060	0.0718	2.214	2.241	2.935
PBE	w/o vdW	3.305	11.326	4.564	0.0935	0.0869	2.224	2.262	3.545
	D2	3.321	10.476	4.426	0.1021	0.0826	2.226	2.261	3.099
	TS	3.309	10.887	4.425	0.0982	0.0826	2.221	2.259	3.306
	optPBE	3.338	10.948	4.541	0.0981	0.0847	2.245	2.282	3.326
	optB88	3.341	10.717	4.468	0.1007	0.0821	2.245	2.281	3.289
	optB86b	3.329	10.513	4.351	0.1029	0.0781	2.238	2.268	3.093

correction should be used for a reliable description of layer-structured systems.

ACKNOWLEDGMENTS

This work has been supported by Sookmyung Women's University through Research Grants 2011.

REFERENCES

[1] C. M. Park and H. J. Shon, Adv. Mater. **19**, 2465 (2007).
[2] A. Morita, Appl. Phys. A **39**, 227 (1986).
[3] H. G. von Schnering, Angew. Chem. Int. Ed. Engl. **20**, 33 (1981).
[4] A. Simon, H. Borrmann and J. Horakh, Chem. Ber-Recl. **130**, 1235 (1997).
[5] H. Okudera, R. E. Dinnebire and A. Simon, Z. Kristallogr. **220**, 259 (2005).
[6] M. Scheer, G. Balázs and A. Seitz, Chem. Rev. **110**, 4236 (2010), and references therein.
[7] P. Hohenberg and W. Kohn, Phys. Rev. **136**, B864 (1964).
[8] W. Kohn and L. J. Sham, Phys. Rev. **140**, B1133 (1965).
[9] M. Elstner, P. Hobza, T. Frauenheim, S. Suhai and E. Kaxiras, J. Chem. Phys. **114**, 5149 (2001).
[10] M. Dion, H. Rydberg, E. Schröder, D. C. Langreth and B. I. Lundqvist, Phys. Rev. Lett. **92**, 246401 (2004).
[11] O. A. von Lilienfeld, I. Tavernelli and U. Rothlisberger, Phys. Rev. Lett. **93**, 153004 (2004).
[12] J. G. Ángyán, I. C. Gerber, A. Savin and J. Toulouse, Phys. Rev. A **72**, 012510 (2005).
[13] A. D. Becke and E. R. Johnson, J. Chem. Phys. **122**, 154104 (2005).
[14] G. Román-Pérez and J. M. Soler, Phys. Rev. Lett. **103**, 096102 (2009).
[15] K. Lee, É. D. Murray, L. Kong, B. I. Undqvist and D. C. Langreth, Phys. Rev. B **82**, 081101(R) (2010).
[16] J. Klimeš, D. R. Bowler and A. Michaelides, J. Phys. Condens. Matter **22**, 022201 (2010).
[17] J. Klimeš, D. R. Bowler and A. Michaelides, Phys. Rev. B **83**, 195131 (2011).
[18] S. Grimme, J. Comp. Chem. **25**, 1463 (2004).
[19] S. Grimme, J. Comp. Chem. **27**, 1787 (2006).
[20] T. Bučko, J. Hafner, S. Lebèfue, and J. G. Ángyán, J. Phys. Chem. A **114**, 11814 (2010).
[21] S. Grimme, J. Antony, S. Ehrlich and H. Krieg, J. Chem. Phys. **132**, 154104 (2010).
[22] A. Tkatchenko and M. Scheffler, Phys. Rev. Lett. **102**, 073005 (2009).
[23] J. C. Slater and J. G. Kirkwood, Phys. Rev. **37**, 682 (1931).
[24] J. Park, B. D. Yu and S. Hong, J. Korean Phys. Soc. **59**, 196 (2011).
[25] S. D. Chakarova-Käck, E. Schröder, B. I. Lundqvist and D. C. Langreth, Phys. Rev. Lett. **96**, 146107 (2006).
[26] M. Hasegawa and K. Nishidate, Phys. Rev. B **70**, 205431 (2004).
[27] J. Y. Noh and H. Kim, J. Korean Phys. Soc. **60**, 410 (2012).
[28] Y. Takao, H. Asahina and A. Morita, J. Phys. Soc. Jpn. **50**, 3362 (1981).
[29] H. Asahina, K. Shindo and A. Morita, J. Phys. Soc. Jpn. **51**, 1193 (1982).
[30] K. J. Chang and M. L. Cohen, Phys. Rev. B **33**, 6177 (1986).
[31] Y. Du, C. Ouyang, S. Shi and M. Lei, J. Appl. Phys. **107**, 093718 (2010).

[32] Ø. Prytz and E. Flage-Larsen, J. Phys.: Condens. Matter **22**, 015502 (2010).
[33] S. Appalakondaiah, G. Vaitheeswaran, S. Lebègue, N. E. Christensen and A. Svane, Phys. Rev. B **86**, 035105 (2012).
[34] J. P. Perdew, J. A. Chevary, S. H. Vosko, K. A. Jackson, M. R. Pederson, D. J. Singh and C. Fiolhais, Phys. Rev. B **46**, 6671 (1992).
[35] A. Brown and S. Rundqvist, Acta Cryst. **19**, 684 (1965).
[36] L. Cartz, S. R. Srinivasa, R. J. Riedner, J. D. Jorgensen and T. G. Worlton, J. Chem. Phys. **71**, 1718 (1979).
[37] J. Heyd, G. E. Scuseria, and M. Ernzerhof, J. Chem. Phys. **118**, 8207 (2003).
[38] C. Adamo and V. Barone, J. Chem. Phys. **110**, 6158 (1999).
[39] G. Kresse and J. Hafner, Phys. Rev. B **47**, 558 (1993).
[40] G. Kresse and J. Hafner, Phys. Rev. B **49**, 14251 (1994).
[41] G. Kresse and J. Furthmüller, Phys. Rev. B **54**, 11169 (1996).
[42] G. Kresse and J. Furthmüller, Comp. Mater. Sci. **6**, 15 (1996).
[43] P. E. Blöchl, Phys. Rev. B **50**, 17953 (1994).
[44] G. Kresse and D. Joubert, Phys. Rev. B **59**, 1758 (1999).
[45] D. M. Ceperley and B. J. Alder, Phys. Rev. Lett. **45**, 566 (1980).
[46] J. P. Perdew, K. Burke and M. Ernzerhof, Phys. Rev. Lett. **77**, 3865 (1996).
[47] H. J. Monkhorst and J. D. Pack, Phys. Rev. B **13**, 5188 (1976).
[48] T. Kikegawa and H. Kwasaki, Acta Cryst. B**39**, 158 (1983).
[49] W. A. Crichton, M. Mezouar, G. Monaco and S. Falconi, Powder Diffr. **18**, 155 (2003).